

## A MATHEMATICAL BACKGROUND

**Definition A.1 (Group)** A group is a set  $G$  equipped with an operator  $*$  such that:

- (closure)  $G$  is closed under  $*$ ; i.e., if  $a, b \in G$ , then  $a * b \in G$
- (identity) There exists an identity element  $e \in G$ ; i.e., for all  $a \in G$  we have  $a * e = e * a = a$
- (inverses) Every element  $a \in G$  has an inverse in  $G$ ; i.e., for all  $a \in G$ , there exists an element  $a' \in G$  such that  $a * a' = a' * a = e$ .
- (associativity) The operator  $*$  acts associatively; i.e., for all  $a, b, c \in G$ ,  $a * (b * c) = (a * b) * c$ .

**Definition A.2 (Group action)** A group action of a group  $G$  on a set  $A$  is a map from  $G \times A \rightarrow A$  (written as  $g.a$ , for all  $g \in G$  and  $a \in A$ ) satisfying the following properties:

- $g_1 \cdot (g_2 \cdot a) = (g_1 \cdot g_2) \cdot a$ , for all  $g_1, g_2 \in G, a \in A$ , and
- $1 \cdot a = a$ , for all  $a \in A$

**Definition A.3 (Representation of a group)** A representation of a group  $G$  on a finite dimensional vector space  $\mathcal{V}$  is a map, from  $G$  to the group of invertible linear operators also called the general linear group  $GL(\mathcal{V})$ :

$$\rho : G \rightarrow GL(\mathcal{V}), \quad (4)$$

which is a homomorphism (Fig. 9 in Appendix C).

$GL(\mathcal{V})$  is the group of symmetries in vector space  $\mathcal{V}$  and its elements are isomorphisms, i.e. invertible transformations, e.g.:  $\forall g \in G, v \in \mathcal{V}$ , the transformation  $T_g : \mathcal{V} \rightarrow \mathcal{V}$  given by  $T_g(v) = g \cdot v$  is a symmetry.

## B PROOF OF THEOREM 3.1

Let  $G$  be the group of symmetries acting on the world state  $\mathcal{W}$  and  $A$  a discrete subgroup of  $G$ . For any  $i \in \{1, \dots, n\}$ , let's consider  $\Psi_i$  to be the map (augmentation) that takes  $x = (x_1, \dots, x_d)^T \in \mathcal{O}$  and returns its image in its corresponding augmented vector space  $\mathcal{V}_i$ .

According to definition [RT], we denote by  $(\rho_0, \mathcal{V})$  the representation of the subgroup  $A_0 \subset G$  containing symmetries of  $\mathcal{O}$  on the agent's latent vector space  $\mathcal{V}$  as discussed in (Fig. 1):

$$\rho_0 : A_0 \subset G \rightarrow GL(\mathcal{V})$$

Let  $P(n)$  be the following statement:

**Statement:** For any  $n \in \mathbb{N}^*$ , the resulting mapping:

$$\tilde{\Psi}_n \doteq \bigoplus_{i=1}^n \Psi_i : \mathcal{O} \longrightarrow \mathcal{O} \bigoplus_{i=1}^n \mathcal{V}_i \cong \tilde{\mathcal{V}}_n,$$

associated with its corresponding representation

$$\tilde{\rho}_n : A \subset G \longrightarrow GL(\tilde{\mathcal{V}}_n),$$

is non-decreasing in total symmetry as  $n$  increases independent of the quality of the  $\Psi_i$  augmentations being used.

We give a proof of the above statement by induction on  $n$ .

**Base case:** Show that the statement holds for  $n = 1$ .

Let's  $\Psi_1$  be the map that takes  $x \in \mathcal{O}$  and returns its corresponding 2D-augmentation in  $M_d^{(1)}(\mathbb{R})$ :

$$\begin{array}{ccc} \Psi_1 : \mathcal{O} & \longrightarrow & M_d^{(1)}(\mathbb{R}) \\ x & \longmapsto & \Psi_1(x) \end{array}$$

where,

$$M_d^{(1)}(\mathbb{R}) = \left\{ \begin{bmatrix} x_1 & s_{i,j}^{(1)}(x) \\ & \ddots \\ & & x_d \end{bmatrix}; \forall i, j \in \{1, \dots, d\} : s_{i,j}^{(1)}(x) \in \mathbb{R} \ \& \ s_{i,i}^{(1)}(x) = x_i \in \mathcal{O} \right\}.$$

We relate the mapping  $\Psi_1$  to the representation  $(\rho_1, M_d^{(1)}(\mathbb{R}))$  associated with the subgroup  $A_1$  of symmetries of type-I:

$$\rho_1 : A_1 \subset G \rightarrow GL(M_d^{(1)}(\mathbb{R}))$$

For any  $x = \begin{bmatrix} x_1 \\ \vdots \\ x_d \end{bmatrix} \in \mathcal{O}$ :

$$\begin{aligned} \Psi_1(x) &= \Psi_1 \begin{pmatrix} x_1 \\ \vdots \\ x_d \end{pmatrix} = \begin{bmatrix} x_1 & & s_{i,j}^{(1)}(x) \\ & \ddots & \\ s_{i,j}^{(1)}(x) & & x_d \end{bmatrix} \\ &= x_1 \begin{bmatrix} 1 & 0 & \cdots & 0 \\ 0 & 0 & & \vdots \\ \vdots & & \ddots & \\ 0 & & & 0 \end{bmatrix} + x_2 \begin{bmatrix} 0 & 0 & \cdots & 0 \\ 0 & 1 & & \vdots \\ \vdots & & \ddots & \\ 0 & & & 0 \end{bmatrix} + \cdots + x_d \begin{bmatrix} 0 & 0 & \cdots & 0 \\ 0 & 0 & & \vdots \\ \vdots & & \ddots & \\ 0 & & & 1 \end{bmatrix} \\ &+ s_{1,2}^{(1)}(x) \begin{bmatrix} 0 & 1 & \cdots & 0 \\ 1 & 0 & & \vdots \\ \vdots & & \ddots & \\ 0 & & & 0 \end{bmatrix} + \cdots + s_{d-1,d}^{(1)}(x) \begin{bmatrix} 0 & 0 & \cdots & 0 \\ 0 & 0 & & \vdots \\ \vdots & & \ddots & \\ 0 & & & 1 \end{bmatrix} \\ &= \text{span} \left\{ \begin{bmatrix} 1 & 0 & \cdots & 0 \\ 0 & 0 & & \vdots \\ \vdots & & \ddots & \\ 0 & & & 0 \end{bmatrix}, \begin{bmatrix} 0 & 0 & \cdots & 0 \\ 0 & 1 & & \vdots \\ \vdots & & \ddots & \\ 0 & & & 0 \end{bmatrix}, \dots, \begin{bmatrix} 0 & 0 & \cdots & 0 \\ 0 & 0 & & \vdots \\ \vdots & & \ddots & \\ 0 & & & 1 \end{bmatrix} \right. \\ &\quad \left. \begin{bmatrix} 0 & 1 & \cdots & 0 \\ 1 & 0 & & \vdots \\ \vdots & & \ddots & \\ 0 & & & 0 \end{bmatrix}, \dots, \begin{bmatrix} 0 & 0 & \cdots & 0 \\ 0 & 0 & & \vdots \\ \vdots & & \ddots & \\ 0 & & & 1 \end{bmatrix} \right\} \end{aligned}$$

which means  $\forall x = (x_1, \dots, x_d)^T \in \mathcal{O}$ , the image of  $\mathcal{O}$  by  $\Psi_1$  can be written in the following form:

$$\Psi_1(\mathcal{O}) = \left. \begin{bmatrix} x_1 \\ \vdots \\ x_d \\ s_{1,2}^{(1)} \\ \vdots \\ s_{d-1,d}^{(1)} \end{bmatrix} \right\} \begin{array}{l} \text{Element of } \mathcal{O} \\ (1D - TS) \\ \\ \text{Could lead to the} \\ \text{emergence of sym-} \\ \text{metries of type-1} \end{array} \cong \text{isomorphic } \mathcal{O} \oplus \mathbb{R} \binom{d^2-d}{2} = \mathcal{O} \oplus \mathcal{V}_1$$

Since the new augmented vector space  $\tilde{\mathcal{V}}_1 \doteq \mathcal{O} \oplus \mathcal{V}_1 \supseteq \mathcal{O}$ , the corresponding representation of the group of symmetries  $A$  on  $\tilde{\mathcal{V}}_1$ :

$$\tilde{\rho}_1 = \rho_0 \oplus \rho_1 : A \subset G \longrightarrow GL(\tilde{\mathcal{V}}_1)$$

is non-decreasing in total symmetry independent of the quality of the augmentation  $\Psi_1$  being used. That is, the statement  $P(1)$  holds true, establishing the base case.

**Inductive step:** Show that for any  $n \geq 1$ , if  $P(n)$  holds, then  $P(n+1)$  also holds.

Assume the induction hypothesis holds, meaning  $P(n)$  is true, and let's verify the statement for  $P(n+1)$ .

Let  $\Psi_1, \dots, \Psi_{n+1}$  be the mappings (augmentations) that take  $x \in \mathcal{O}$  and return their corresponding 2D-augmentation in  $M_d^{(1)}(\mathbb{R}), \dots, M_d^{(n+1)}(\mathbb{R})$  respectively.  $\forall i \in \{1, \dots, n+1\}$ , the image of  $\mathcal{O}$  by any augmentation  $\Psi_i$  can be written as:

$$\Psi_i(\mathcal{O}) = \left[ \begin{array}{c} x_1 \\ \vdots \\ x_d \\ s_{1,2}^{(i)}(x) \\ \vdots \\ s_{d-1,d}^{(i)}(x) \end{array} \right] \left. \begin{array}{l} \text{Element of } \mathcal{O} \\ (1D - TS) \\ \\ \text{Symmetries} \\ \text{of type-}i \end{array} \right\} \cong_{\text{isomorphic}} \mathcal{O} \oplus \mathbb{R}^{\binom{d^2-d}{2}} = \mathcal{O} \oplus \mathcal{V}_i$$

Since the direct sum of vector spaces is also a vector space then:

$$\begin{aligned} \bigoplus_{i=1}^{n+1} M_d^{(i)}(\mathbb{R}) &= M_d^{(1)}(\mathbb{R}) \oplus M_d^{(2)}(\mathbb{R}) \oplus \dots \oplus M_d^{(n)}(\mathbb{R}) \oplus M_d^{(n+1)}(\mathbb{R}) \\ &\stackrel{\text{iso}}{\cong} \left[ \mathcal{O} \oplus \mathcal{O} \oplus \dots \oplus \mathcal{O} \right] \oplus \mathcal{V}_1 \oplus \mathcal{V}_2 \oplus \dots \oplus \mathcal{V}_n \oplus \mathcal{V}_{n+1} \\ &\begin{array}{l} \searrow \\ \text{since } [\mathcal{O} \oplus \mathcal{O} \oplus \dots \oplus \mathcal{O}] \\ \text{doesn't add new symmetries} \end{array} \\ &\stackrel{\text{iso}}{\cong} \underbrace{\mathcal{O}}_{ID-TS} \oplus \mathcal{V}_1 \oplus \mathcal{V}_2 \oplus \dots \oplus \mathcal{V}_n \oplus \underbrace{\mathcal{V}_{n+1}}_{\text{sym. of type-}n+1} \\ &\begin{array}{l} \searrow \\ \mathcal{O} \oplus_{i=1}^n \mathcal{V}_i \doteq \tilde{\mathcal{V}}_n \supseteq \tilde{\mathcal{V}}_{n-1} \\ \text{(induction hypothesis)} \end{array} \\ &= \tilde{\mathcal{V}}_n \oplus \mathcal{V}_{n+1} \end{aligned} \tag{5}$$

Since the new augmented vector space  $\tilde{\mathcal{V}}_{n+1} \doteq \tilde{\mathcal{V}}_n \oplus \mathcal{V}_{n+1} \supseteq \tilde{\mathcal{V}}_n$ , the corresponding representation of the group of symmetries  $A$  on  $\tilde{\mathcal{V}}_{n+1}$ :

$$\tilde{\rho}_{n+1} \doteq \bigoplus_{i=1}^{n+1} \rho_i : A \subset G \longrightarrow GL(\tilde{\mathcal{V}}_{n+1})$$

is non-decreasing in total symmetry independent of the quality of the augmentations  $\Psi_i$  being used for any  $i \in \{1, \dots, n+1\}$ . That is, the statement  $P(n+1)$  also holds true, establishing the inductive step.

**Conclusion:** Since both the base case and the inductive step have been proved as true, by mathematical induction the statement  $P(n)$  holds for any  $n \in \mathbb{N}^*$ .

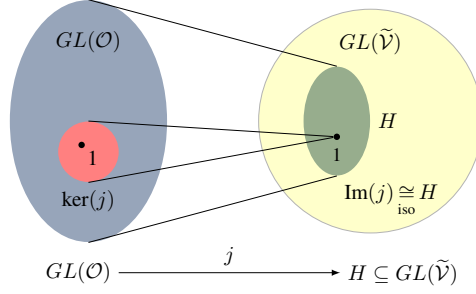
## C PROOF OF COROLLARY 3.1

According to (Eq. 5) in the proof of theorem 3.1, we have  $\mathcal{O} \subseteq \tilde{\mathcal{V}}$  by construction.

Our goal is to proof that the group of symmetries of the augmented vector space  $\tilde{\mathcal{V}}$  denoted by  $GL(\tilde{\mathcal{V}})$  is necessarily larger than the group of symmetries of  $\mathcal{O}$  denoted by  $GL(\mathcal{O})$ .

Mathematically, this means that we need to demonstrate that  $GL(\mathcal{O})$  is a subgroup of  $GL(\tilde{\mathcal{V}})$ , *i.e.* that is:  $GL(\mathcal{O}) \subseteq GL(\tilde{\mathcal{V}})$ .

Let's consider  $A \in GL(\tilde{\mathcal{V}}) \subseteq \text{End}(\tilde{\mathcal{V}})$ . This inclusion is trivial since the set of endomorphisms always includes the set of automorphisms.


 Figure 9: Image of a group homomorphism  $j$ .

According to (Eq. 5) and the property of decomposition of endomorphisms, we have:

$$A = \begin{bmatrix} A_0 & A_{0 \rightarrow 1} & \cdots & A_{0 \rightarrow n} \\ & A_1 & & \\ & & \ddots & \\ & & & A_n \end{bmatrix}$$

The endomorphism (matrix)  $A$  is a block diagonal matrix and it contains  $n + 1$  diagonal blocks if  $n$  augmentations are being used.

To prove that  $GL(\mathcal{O}) \subseteq GL(\tilde{\mathcal{V}})$ , it suffices to consider a sub-group of  $GL(\tilde{\mathcal{V}})$  named  $H$  and to show that  $H$  is isomorphic to  $GL(\mathcal{O})$ .

To do so, let's consider the following group homomorphism  $j$ :

$$j : \begin{array}{ccc} GL(\mathcal{O}) & \longrightarrow & H \subset GL(\tilde{\mathcal{V}}) \\ A_{\mathcal{O}} & \longmapsto & j(A_{\mathcal{O}}) \end{array} \quad (6)$$

where:

$$j(A_{\mathcal{O}}) = \begin{bmatrix} A_{\mathcal{O}} & 0 & 0 & 0 \\ 0 & \mathbb{1} & 0 & 0 \\ 0 & 0 & \ddots & 0 \\ 0 & 0 & 0 & \mathbb{1} \end{bmatrix}$$

Showing that the homomorphism  $j$  is injective guarantees that  $GL(\mathcal{O}) \underset{\text{iso}}{\cong} H \subset GL(\tilde{\mathcal{V}})$ .

Now we will call upon two properties of group homomorphisms:

**Proposition C.1** *Let  $G$  and  $H$  be groups and let  $\varphi : G \rightarrow H$  be a homomorphism.*

*$\text{Im}(\varphi)$ , the image of  $G$  under  $\varphi$  is a subgroup of  $H$  and we write:*

$$\text{Im}(\varphi) \underset{\text{iso}}{\cong} \frac{H}{\ker(\varphi)}$$

*where  $\ker(\varphi)$  denotes the kernel of  $\varphi$ .*

**Definition C.1** *If  $\varphi$  is a homomorphism  $\varphi : G \rightarrow H$ , the kernel of  $\varphi$  is the set  $\{g \in G \mid \varphi(g) = \mathbb{1}_H\}$  and will be denoted by  $\ker \varphi$ . So the kernel is the set of elements in  $G$  which map to the identity of  $H$ , i.e., is the fiber over the identity of  $H$ .*

**Proposition C.2** *If the kernel of a group homomorphism  $\varphi : G \rightarrow H$  is set to be equal to the identity  $\ker(\varphi) = \mathbb{1}_G$ , then  $\varphi$  is injective.*

Now going back to the group homomorphism defined in (Eq. 6):

By proposition C.1:

$$\text{Im}(j) \underset{\text{iso}}{\cong} \frac{H}{\ker(j)}$$

Additionally, the only one way to get  $\text{Im}(j) = \mathbb{1}_H$  is when  $A_{\mathcal{O}}$  is the identity ( $A_{\mathcal{O}} = \mathbb{1}$ ), which by proposition C.2 implies that  $j$  is injective.

Considering the two proposition C.1 and C.2 together, we have:

$$j(A_{\mathcal{O}}) \in \text{Im}(j) \underset{\text{iso}}{\cong} \frac{H}{\ker(j)} \underset{\text{iso}}{\cong} H \subset GL(\tilde{\mathcal{V}})$$

i.e.

$$j\left(GL(\mathcal{O})\right) \underset{\text{iso}}{\cong} H \subset GL(\tilde{\mathcal{V}})$$

Thus, by considering the augmented representation  $\rho_{\text{ISSA}}$ , we have proved that we necessarily have more symmetries in the augmented vector space  $\tilde{\mathcal{V}}$  compared to  $\mathcal{O}$ . This allows the RL agent to perform at least as good when using the original  $1D - TS$  representation  $\rho_0$ .

## D DATASET, SETUP, AND POLICY DEPLOYMENT

### D.1 DATASET

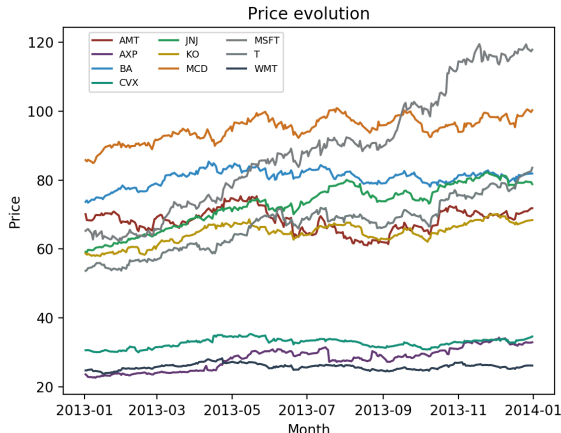


Figure 10: Evolution of stock prices.

The data comes from the Quandl finance database that has daily data. Our dataset includes January 1<sup>st</sup> 2013 up to December 31<sup>st</sup> 2013, resulting in 252 trading days (Fig. 10). The RL agents rebalance the portfolio on a daily basis and are evaluated on a portfolio consisting of the following ten selected securities: American Tower Corp. (AMT), American Express Company (AXP), Boeing Company (BA), Chevron Corporation (CVX), Johnson & Johnson (JNJ), Coca-Cola Co (KO), McDonald’s Corp. (MCD), Microsoft Corporation (MSFT), AT&T Inc. (T) and Walmart Inc (WMT). To promote the diversification of the portfolio, these stocks were selected from different sectors of the S&P 500, so that they are uncorrelated as much as possible as shown in Fig. 10 above.

It should be noted that for noisy dynamical systems, the test sets are commonly much smaller than the training sets compared to static data because errors accumulate over longer test windows. For our experiments we used 200 samples for training and 50 samples for testing with a testing window of 10 samples (2 weeks). We found two weeks to be the largest practical testing window.

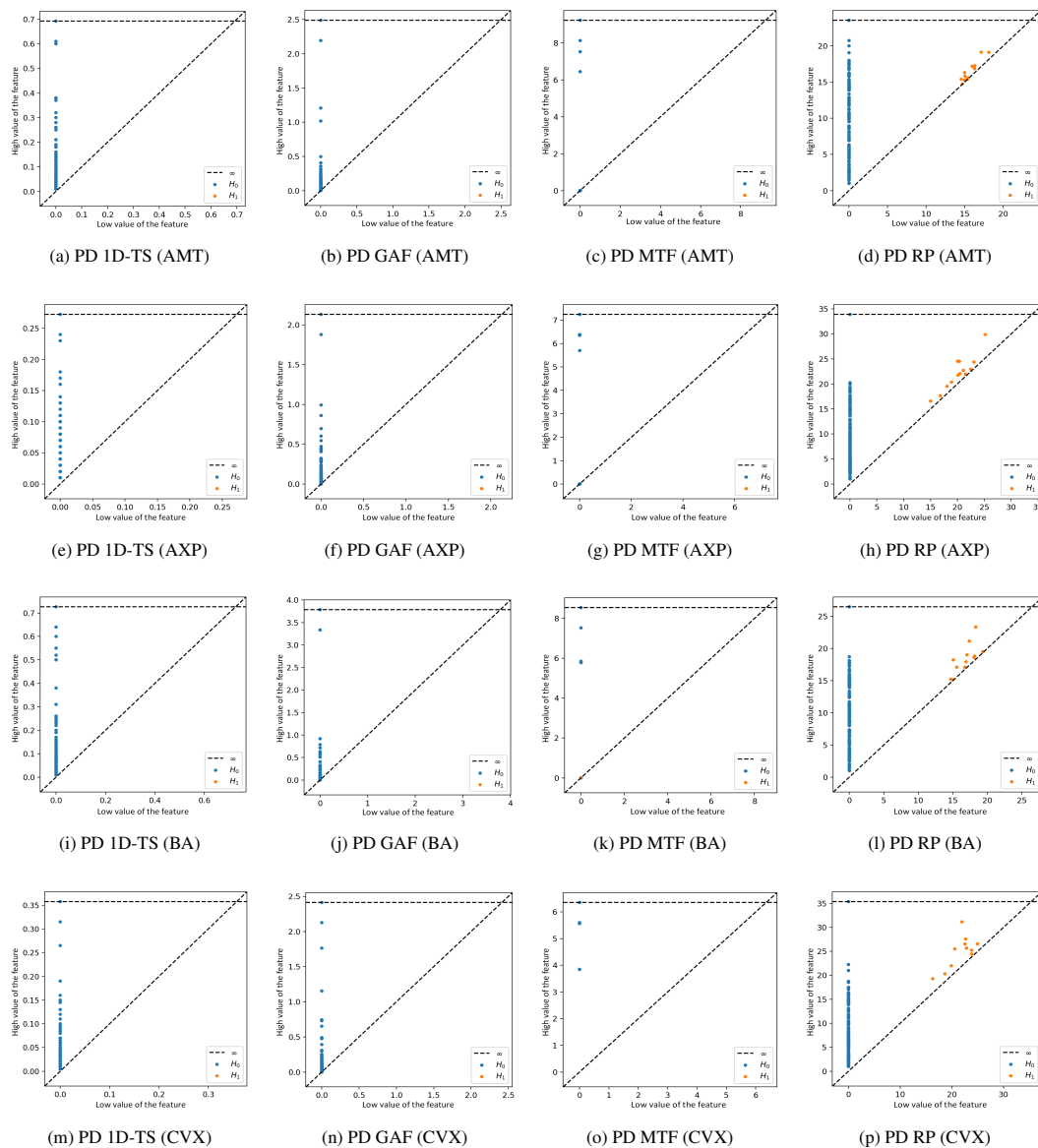
### D.2 SETUP

Experiments were run on a 24-core machine with 33GB of memory. All algorithms were implemented in Python using Keras and Tensorflow libraries. Each method is executed in an asynchronously parallel set up of 2 GPUs, that is, it can evaluate multiple models in parallel, with each model on a single GPU. When the evaluation of one model finishes, the methods can incorporate the result and immediately re-deploy the next job without waiting for the others to finish. We use 2 NVIDIA Quadro P5000 (16GB) GPUs.

### D.3 POLICY DEPLOYMENT

In our experiments, the investment decisions are made daily and each input signal represents a multidimensional tensor that aggregates historical open, low, high, close prices and volume. Our deep RL models are trained and tested using a sliding window allowing the agents to adapt to new market conditions. The models are trained and tested using 5 successive rounds with a shift of 10 days between rounds. Each round consists of a training period of 200 days followed by a 10 day testing period. We found a 10 day testing window to be the largest window size appropriate for daily frequency data. In fact, the volatility of the market is a major concern in most ML-based trading systems. It should be noted that our training and testing include the transaction costs (TC). We used the typical cost due to bid-ask spread and market impact that is 0.25%. We believe these are reasonable transaction costs for the portfolio trades.

#### D.3.1 PERSISTENCE DIAGRAMS



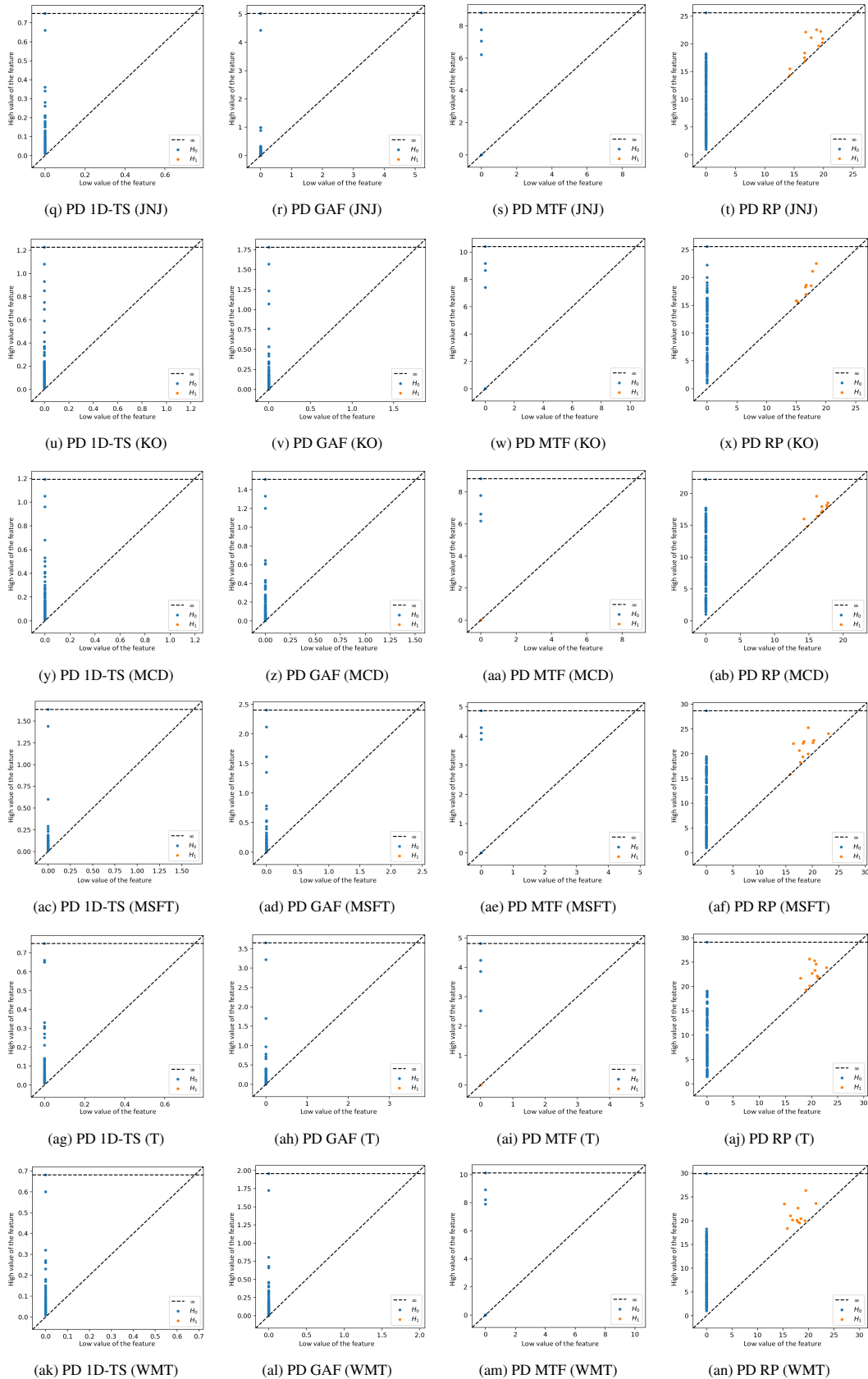


Figure 11: Persistence diagrams for the 10 stocks in our portfolio

## D.4 HYPERPARAMETERS

Table 4: Range of hyperparameters for the CNN-RL case study

Parameters	Search space	Type
Learning rate	$10^{-5}$ - $5 \cdot 10^{-1}$	Discrete
Window	10 - 30	Discrete
Number of filters	2 - 52	Discrete
Kernel Strides	2 - 10	Discrete
Number of units per layer	50 - 1000	Discrete
Optimizer	0 : Adam 1 : Adadelata 2 : Adagrad	Categorical

Table 5: Convolution and dense layers for the supervised learning case study

Layer (type)	Output Shape	Param #
conv2d_192 (Conv2D)	(None, 126, 126, 32)	608
batch_norm_1 (BatchNormaliza)	(None, 126, 126, 32)	128
leaky_re_lu_192 (LeakyReLU)	(None, 126, 126, 32)	0
max_pooling2d_192 (MaxPoolin)	(None, 63, 63, 32)	0
conv2d_193 (Conv2D)	(None, 61, 61, 32)	9248
batch_norm_2 (BatchNormaliza)	(None, 61, 61, 32)	128
leaky_re_lu_193 (LeakyReLU)	(None, 61, 61, 32)	0
max_pooling2d_193 (MaxPoolin)	(None, 30, 30, 32)	0
flatten_96 (Flatten)	(None, 28800)	0
dense_192 (Dense)	(None, 128)	3686528
dense_193 (Dense)	(None, 3)	387

## D.5 SAMPLE EFFICIENCY GAINS DUE TO SYMMETRY AUGMENTATIONS (FIG.5)

Table 6: Summary of results of the best DPG model with various augmentations.

Agent performance	Cumulative return	Average value	STD value	Max value	Min value
dpg dense 1D-TS	3.0473	2.3418	0.9230	4.0716	1.0
dpg dense GAF	3.4016	2.3762	1.0052	4.4262	1.0
dpg dense MTF	3.6808	2.5853	1.1141	4.7137	1.0
dpg dense GAF+MTF	3.9046	2.6046	1.1462	4.9305	1.0

Table 7: Summary of results of the second best DPG model with various augmentations.

Agent performance	Cumulative return	Average value	STD value	Max value	Min value
dpg dense 1D-TS	2.8217	2.2454	0.8495	3.8649	1.0
dpg dense GAF	3.0157	2.2975	0.9172	4.0572	1.0
dpg dense MTF	3.0317	2.3356	0.9211	4.0691	0.9997
dpg dense GAF+MTF	3.3846	2.4666	1.0206	4.4131	1.0

Table 8: Summary of results of the best PPO model with various augmentations.

Agent performance	Cumulative return	Average value	STD value	Max value	Min value
ppo dense 1D-TS	0.0939	1.0674	0.0445	1.1301	0.9720
ppo dense GAF	0.2385	1.1636	0.0786	1.2696	1.0
ppo dense MTF	0.6713	1.3960	0.2221	1.7004	1.0
ppo dense GAF+MTF	0.8898	1.4595	0.2703	1.9183	1.0

Table 9: Summary of results of the second best PPO model with various augmentations.

Agent performance	Cumulative return	Average value	STD value	Max value	Min value
ppo dense 1D-TS	0.0473	1.0391	0.0319	1.0906	0.9721
ppo dense GAF	0.0757	1.0582	0.0346	1.1154	0.9841
ppo dense MTF	0.0810	1.0651	0.0376	1.1238	0.9896
ppo dense GAF+MTF	0.2158	1.1120	0.0670	1.2314	0.9854

## D.6 TESTING DEMONSTRATES GENERALIZATION WITH POTENTIAL OVERFITTING (FIG.6)

Table 10: Summary of DPG training results with various augmentations.

Agent performance	Cumulative return	Average value	STD value	Max value	Min value
dpg dense 1D-TS	-0.0359	0.9971	0.0219	1.0293	0.9366
dpg RP+GAF+MTF	0.0413	1.0404	0.0267	1.0858	0.9765
dpg dense RP+GAF+MTF	0.6363	1.2785	0.1948	1.6401	0.9930

Table 11: Summary of DPG testing results with various augmentations.

Agent performance	Cumulative return	Average value	STD value	Max value	Min value
dpg dense 1D-TS	0.0181	1.0098	0.0110	1.0231	0.9879
dpg RP+GAF+MTF	0.0209	1.0109	0.0114	1.0236	0.9884
dpg dense RP+GAF+MTF	0.0304	1.0073	0.0133	1.0304	0.9857

Table 12: Summary of PPO training results with various augmentations

Agent performance	Cumulative return	Average value	STD value	Max value	Min value
ppo dense 1D-TS	-0.1662	0.9274	0.0499	1.0222	0.8188
ppo RP+GAF+MTF	0.0477	1.0450	0.0279	1.0918	0.9810
ppo dense RP+GAF+MTF	0.0739	1.1046	0.0673	1.2201	0.9618

Table 13: Summary of PPO testing results with various augmentations

Agent performance	Cumulative return	Average value	STD value	Max value	Min value
ppo dense 1D-TS	-0.0193	0.9946	0.0122	1.0236	0.9806
ppo RP+GAF+MTF	0.0217	1.0112	0.0116	1.0235	0.9884
ppo dense RP+GAF+MTF	0.0128	1.0132	0.0195	1.0429	0.9819

## E ACCURACY FOR CBF

Table 14: Test accuracy for CBF with various augmentations.

Trials	RP	MTF	GAF	RP+MTF	RP+GAF	MTF+GAF	RP+MTF+GAF
1	0.8144	0.3311	0.3766	0.9011	0.8933	0.5966	0.9433
2	0.4755	0.3311	0.4811	0.8122	0.9288	0.5411	0.9244
3	0.5600	0.3311	0.5922	0.9077	0.7444	0.6177	0.9355
4	0.8033	0.3466	0.4666	0.6377	0.8333	0.4	0.8133
5	0.8066	0.3311	0.4355	0.7233	0.8988	0.37	0.8944
6	0.7988	0.3377	0.3477	0.8077	0.8199	0.4088	0.8588
7	0.8566	0.6511	0.3855	0.7588	0.7144	0.4477	0.9344
8	0.5099	0.5166	0.6455	0.8088	0.8222	0.7411	0.8566
9	0.9377	0.5899	0.9222	0.9333	0.9255	0.9533	0.9522
10	0.7655	0.5677	0.8944	0.9355	0.9077	0.8799	0.9499
<b>Average</b>	<b>0.7492</b>	<b>0.4686</b>	<b>0.5891</b>	<b>0.8313</b>	<b>0.8574</b>	<b>0.6282</b>	<b>0.9112</b>